PERFORMANCE EVALUATION OF NANOFLUID ON PARABOLIC TROUGH SOLAR COLLECTOR

Vijayan GOPALSAMY[1*], Karunakaran RAJASEKARAN[2]

[1]Research Scholar, Department of Mechanical Engineering,

Anna University-Chennai, Tamilnadu 600 025, India

[2]Professor, Department of Mechanical Engineering, UCE-Kanchipuram,

Anna University-Chennai, Tamilnadu 600 025, India

[*] Corresponding author; E-mail: viji_laker@yahoo.co.in

In the present work, the performance of aluminum oxide (Al_2O_3) and deionized (DI) water nanofluid used as heat transfer fluid on a parabolic trough solar collector (PTSC) system with hot water generation tank is evaluated. The parabolic trough solar collector is developed using easily and locally accessible materials. Five different concentrations of aluminum oxide and deionized water based nanofluid from 0.5 to 2.5% is prepared by the magnetic stirrer initially and then the mixture is subjected to ultrasonication process to break aggregates with the absence of surfactant. The prepared nanofluids are allowed to flow through the absorber which is located at a focal point of the solar collector. The performance of nanofluid is compared with pure deionized water. The test is conducted from 8.00 am to 16.00 pm daily in the whole length of the test span. The heat transfer fluid is allowed to flow at a mass flow rate of 0.020 kgs^{-1} and 0.09246 ms^{-1} velocities. The maximum solar radiation is 821 Wm^{-2}, and maximum efficiency is observed at noon time 60.41% for deionized water and 60.49% for 2.5% volumetric fraction of alumina nanofluid. The efficiency enhancement was 3.90% than deionized water. The influence of the critical parameter on the performance is also examined.

Key words*: Parabolic trough solar collector, Alumina, Deionized water, Nanofluid, Volume fraction, Rim angle*

1. Introduction

The parabolic trough solar concentrator system is used for unique fields such as power production [1,2], steam and hot water generation for the domestic purpose [3,4]. The possibilities of producing hot water using PTSC were discussed. Research work so far done proves that the PTSC holds good for hot water generation when compared with the non-concentrating type of solar collector. The concentrated type solar collector of conical geometry was also used for hot water production [5]. The parabolic trough solar collector was used for domestic power generation purpose using the stirling cycle, where water was used as a heat transfer fluid [6]. Many researchers investigated the

performance of nanofluid on parabolic trough concentrator, instead of using water as a working fluid and they compared the performance [7]. Nanosized solid particles mixed in liquid, are known as nanofluid, was used in the solar collector. Many research works were carried out to analyze the performance of nanofluid of various types and volume fractions on parabolic trough solar collector. They detailed the list of various heat transfer fluids such as synthetic oil, therminol VP-I, nitrate salt:395°C, ionic liquid:459°C, CO_2:480°C and sulphur: 490°C which can be used depending upon the working temperature, operation aspects, storage aspects, safety aspects and cost on parabolic trough solar thermal power plant [8]. The therminol VP-I, nitrate molten salt, sodium liquid, air, carbon monoxide, pressurized water, and helium can also be applied as heat transfer fluids [9]. The author constructed a standard pilot model of parabolic trough collector of with four kinds of receiver namely black painted vacuumed steel pipe, bare copper tube coated with black chrome coating, non-evacuated glass tube and vacuumed copper tube with a black coating. The carbon nanotubes of 0.2 and 0.3% volume fraction were dispersed into the oil to use as working fluid [10-12]. The author used distilled water based multi-wall carbon nanotube and potassium persulfate as an oxidant. The nanofluid was prepared with the volume concentrations of 49.9 to 50.1 mg per litre of distilled water for balancing pumping power. The collector efficiency enhances from 54 to 73% when using multiwall carbon nanotubes in a glass tube receiver and operating temperature increases from ambient to 80°C [13]. The author analyzed the forced convection heat transfer of CuO/water and Al_2O_3/water nanofluid subjected to flow through the receiver tube of the parabolic trough solar collector numerically [14]. The author used monte-carlo ray tracing (MCR) method to investigate the effect of rotational and irrotational of the LS-2 Luz collector on fluid outlet temperature and heat gain, where syltherm-800 was used as heat transfer fluid. The result proved the rotation of collector has a positive effect [15].

Many authors analyzed and compared the experimental output with the results obtained from the simulation and other analysis techniques. Numerical [16-19], experimental [20,21], simulation, numerical [22], analytical [23], modeling, heat transfer analysis work [16,24] and modeling cum optimization [25,26] were carried out for the purpose of evaluating their results. The author carried out the modeling of parabolic trough solar collector with a well-mixed hot water storage tank. They developed the model, and its results were verified with experimental work. The hot water temperature deviation between predicted and actual is 9.59% only [27]. The author designed the solar dish collector by solidworks software, to analyze both in optical and thermal mode. Maximum optical efficiency is obtained at 2.1 m focal length and exergetic efficiency is varied from 4 to 15% depending upon the inlet water temperature [28]. They investigated the effect of solar radiation on various performance parameters of parabolic trough solar collector at a different time [29]. The author developed two hybrid solar collectors with the photovoltaic panel, one fixed above the absorber and other located on the absorber itself to investigate the conversion ability of solar radiation into heat and /or electricity [30]. Extensive research work in synthesizing of distinctive types of nanofluid at various volume fractions either by one step or two-step method was done. Properties of nanofluid were evaluated, and the performance enhancement was analyzed while using the absorber of the parabolic trough solar collectors [31-33].

In this present work, the performance of the parabolic trough solar collector is investigated experimentally while the aluminum oxide/deionized water nanofluid of various volume fractions is subjected to flow through it. Both the fabrication of PTSC and preparation of alumina nanofluid are done in the lab. Most of the work carried out so far on PTSC, using nanofluid as heat transfer fluid

was with shielded type receiver and incurred a high cost. Only very few works were done on the unshielded receiver with nanofluid. So an attempt has been made to develop the low-cost unshielded receiver type PTSC by utilizing the locally available materials.

2. Experimental platform

2.1. Parabolic trough solar collector system

The present research work includes two parts: 1) fabrication of a parabolic trough solar collector; 2) preparation of alumina and deionized water nanofluid. Fabrication of the PTSC system and preparation of alumina/deionized water nanofluid are done in the lab.

A new low-cost parabolic trough solar concentrator with hot water production system is developed for this research work. The total cost of the system is around 390 USD. The complete system includes: 1) aperture-to reflect the solar radiation; 2) absorber-to absorb the radiation reflected from the reflector (aperture) surface and transferring the heat energy to heat transfer medium; 3) heat energy storage system-to transfer the heat energy of nanofluid to water through heat exchanger which is kept in the heat energy storage tank; 4) nanofluid tank-to store the nanofluid; 5) mini submersible pump-to circulate nanofluid which is placed inside the nanofluid tank. The parabolic geometry [34,35] is developed by an Eq. (1) and the calculated rim angle is 73.74° as shown in Fig.1. The parabolic curvature is fabricated by mild steel sheet as per the accurately calculated value. The locally available plane mirror (τ=0.97) of striped shape is fixed on the curvature to complete the reflector part, which reflects the incident solar rays equal to the angle of incidence. The selection of the reflector is based on the availability, reflectivity, and cost. The sketch of the experimental set up is shown in Fig. 2, and the detailed specifications are given Tab. 1.

$$X^2 = 4ay \qquad (1)$$

Figure 1. Parabolic structure

The collector is kept on an open terrace (Longitude: 79.3881°E, Latitude: 10.9617°N) oriented north-south direction and tracked manually in east-west. Tracking was monitored for every 5-minutes in such a way to receive maximum radiation. The test was carried out from 8.00 am to 4.00 pm every day for six values of concentration and 0.02 kg/s of mass flow rate. The copper tube is selected as the receiver due to its high thermal conductivity, and it is painted black to absorb the solar radiation utmost. The receiver is aligned at a calculated focal point to face the solar radiation from the reflector surface always. Both the absorber and aperture are supported by a sturdy mild steel structure. The PTC is oriented in the north-south direction and tracking was carried out manually in east-west at an angle of 15° per hour, to be in the limelight of the solar radiation always. The temperature indicator is used to sense the nanofluid inlet temperature, nanofluid outlet temperature, absorber surface temperature, ambient temperature, and heat energy storage tank fluid temperature. A mini submersible pump kept in the nanofluid tank is used to circulate the nanofluid continuously through the receiver, heat energy storage tank and finally to the nanofluid tank at a defined mass flow rate, to complete the fluid circuit. The rotameter is connected at the entry side of the receiver to control the mass flow rate of nanofluid.

Table 1. Specifications of PTSC

Parameter	Design value
Collector length (mm)	1200
Collector width (mm)	900
Absorber inner diameter (mm)	16.6
Absorber outer diameter (mm)	17.2
Aperture area (m^2)	1.08
Focus length (mm)	300
Mirror radius (degree)	474
Local mirror radius (degree)	346.5
Rim angle (degree)	73.74
Minimum image diameter (mm)	4.418
Energy storage tank (litre)	15
Nanofluid tank (litre)	5
Mass flow rate (kgs^{-1})	0.020
Concentration ratio (CR)	16.34
Reflectivity	0.97
Intercept factor	0.91
Absorptance	0.90

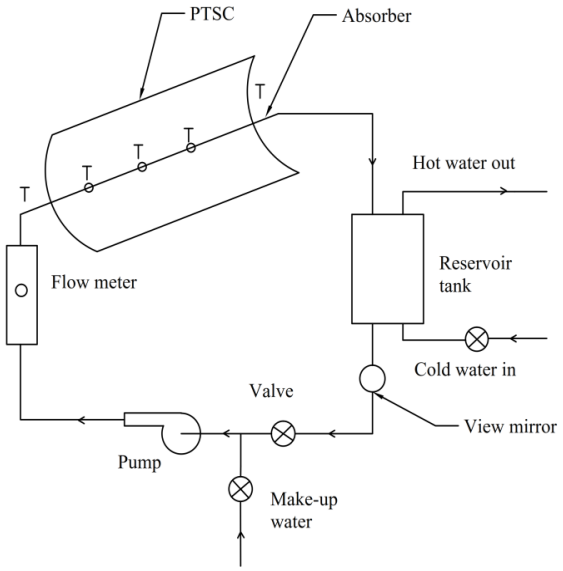

Figure 2. Sketch of PTS collector

2.2. Preparation of nanofluid

Nanofluid is prepared by a two-step method. In this method first nanoparticles are prepared then it is mixed with the base fluid. In our work, the Al_2O_3 nanoparticles are bought from M/s. Alfa Asear, and it is mixed with DI water without surfactant presence. The properties of nanoparticle are given in Tab. 2. The required quantity of nanoparticle for preparing the nanofluid is calculated as per the Eq. (2) and weight of the particles required per 1000 ml presented in Tab. 3. *Actually, it is the ratio of the volume of nanoparticle (v_{np}) to the sum of the nanoparticle volume and the base fluid volume (v_{bf}). The Fig. 3 and 4 show the nanofluid preparation equipment.* The calculated quantity of alumina particles is weighed by an electronic weighing machine. *First,the alumina nanoparticles are diluted in DI water using magnetic stirrer, which is operated at a speed of 500 revolutions per minute for the period of 30 minutes. Then the mixture is subjected to ultrasonication process for 60 minutes, It is an approved and commonly used technique for nanofluid preparing.* Various volume fractions of nanofluid are prepared such as 0.5, 1.0, 1.5, 2.0 and 2.5%, each of 5000 ml per concentration, to act as heat transfer fluid and to complete the nanofluid cycle.

$$W_{np} = \left[V_{np} \Big/ V_{np} + V_{bf} \right] \tag{2}$$

Figure 3. Magnetic stirrer

Figure 4. Ultrasonic bath

Table 2. Specifications of Nanoparticle

Chemical name	Aluminum oxide	Appearance	White
Formula	Al_2O_3	Surface area	32-40 m^2g^{-1}
Make	NanoDur	Density	3.72 gcm^{-3}
Phase	Solid	Melting	2045^oC
Shape	Sphere	Boiling	2980^oC
Form	Powder	C_p	765 $Jkg^{-1}K^{-1}$
Purity	99.5%	K	40 $Wm^{-1}K^{-1}$

Table 3. Weight of np/1000ml

Concentration (%)	Weight (g)
0.5	18.6
1.0	37.2
1.5	55.8
2.0	74.4
2.5	93.0

3. Performance tests

The experimental work is carried out on the collector system as shown in Fig. 5, and the efficiency of the system is determined from the obtained values. The instantaneous efficiency for different solar radiation intensity, ambient temperature, nanofluid inlet temperature, and wind velocity are measured. The absorbed solar radiation depends on the reflectivity of aperture material, therefore the collector surface having good reflectance property will reflect almost all the radiation which is falling on the surface and it can be calculated [36-38] as per Eq. (3). Both wind loss and radiation loss influences the heat coefficient and can be calculated by Eq. (4). Wind loss coefficient is affected by wind velocity, ambient temperature, and absorber surface temperature which are dominating parameters.

$$S = I_b R_b \rho\gamma(\tau\alpha) + I_b R_b (\tau\alpha)\left(D_o / W + D_o\right) \tag{3}$$

$$U_l = \left[\left(1/h_w\right) + \left(1/h_r\right)\right]^{-1} \tag{4}$$

For the nanofluid flowing inside the tube, first, the bulk mean temperature is calculated. Then, the properties such as density, kinematic viscosity, dynamic viscosity, specific heat, prandtl number, and thermal conductivity are to be taken from their thermo-physical property data at bulk mean

temperature which is calculated experimentally. To confirm whether the flow is laminar or turbulent, the value of Re is calculated. If the value of $Re < 2300$, then the flow is laminar so that the flow is coming under fully developed hydrodynamic and thermal profile mode. Therefore, $Nu = 3.7$ is considered for constant wall temperature [34]. If the value is in the range of $2300 < Re < 5 \times 10^6$ and $0.5 < Pr < 2000$, then the nanofluid flowing inside the receiver tube ensures the region of fully developed turbulent flow. The Eq. (5,6) represented by Gnielinski is used to calculate the friction factor and Nu for turbulent flow.

Figure 5. Experimental set-up

$$f = \left(1.58 \times \ell n(\mathrm{Re}) - 3.28\right)^{-2} \tag{5}$$

$$Nu = \frac{\left(f/2\right)(\mathrm{Re}-1000)\mathrm{Pr}}{1.0 + 12.7\left(\sqrt{f/2}\right)\left(\mathrm{Pr}^{2/3}-1\right)} \tag{6}$$

There is no variation in the receiver tube dimension and its thermal conductivity, the heat loss coefficient and inside heat transfer co-efficient dominated the overall heat loss coefficient given in Eq. (7).

$$U_o = \left[\left(1/U_l\right) + \left(D_o/\left(D_i \times h_{fi}\right)\right) + \left(D_o/2K_r\right)\ell n\left(D_o/D_i\right)\right]^{-1} \tag{7}$$

The actual useful heat gain is the difference between useful heat gain and total heat loss and is determined by the Eq. (8) and the instantaneous collector efficiency is proportional to the actual useful heat gain available and it is the ratio of useful heat gain and heat available from the aperture area. It can be determined from Eq. (9).

$$Q_u = F_R A_a \left(S - \left(1/CR\right)\right) U_o \left(T_{fi} - T_a\right) \tag{8}$$

$$\eta_{ins} = \left[Q_u/\left(I_b R_b W L\right)\right] \tag{9}$$

Now the optical efficiency is determined for the various incident angle of solar radiation by Eq. (9). The optical efficiency (η_{opt}) only depends on the reflectivity (ρ) of aperture material, intercept factor (γ), the transmittance-absorptance product of the receiver ($\tau\alpha$). Both the incident angle modifier and end loss were also taken in to account as shown in Eq. (10) while calculating the optical efficiency.

$$\eta_{opt} = \left(\rho\gamma\tau\alpha\right) \times K(\theta) \times \left(X_{endloss}\right) \tag{10}$$

The transmittance parameter can be omitted due to unshielded type receiver. The inlet temperature of nanofluid and an outlet temperature of nanofluid, ambient temperature, and the water temperature are observed using PT-100 resistance temperature detector. The Solar power meter, vane type anemometer, and rotameter are used to measure the beam radiation, wind speed, and mass flow rate respectively along with the instrument details in Tab. 4. Each concentration was tested for three days. Before charging the next concentration, the existing nanofluid is fully drained. To complete the cleaning process the test run was conducted with deionized water, and then the system is kept in ideal condition. All these parameters are observed at every five minutes time interval. The parametric values measured using the instruments discussed here have not deviated over the limit specified by the ASHRAE standard which confirms that the experimental works are under steady state condition and considering the uncertainty of the measuring instruments, in mind, the experimental error was calculated as 2.06%.

Table 4. Details of instrumentation

Parameter	Instrument	Model	Accuracy
Solar radiation	Solar power meter	TM 207	± 10 Wm^{-2}
Wind speed	Vane probe anemometer	AVM 07	±2% + 0.1 ms^{-1}
Ambient temperature			0.5°C
Temperature	RTD	PT 100	± [0.15+0.02(t)]°C

4. Results and discussion

The variation of ambient temperature, bulk mean temperature and surface temperature during the whole testing period is shown in Fig. 6. It attained highest receiver temperature of 139.82°C, and the bulk mean temperature at that time is 42.67°C which is the maximum value of testing hour in a day, from 8.00 am to 4.00 pm. These three temperatures are purely depended on solar radiation and it increased with radiation and wind velocity. Low wind velocity and high solar radiation offered the fruitful result in terms of higher receiver temperature which is the reason for the increase in the outlet temperature of the nanofluid. But at the same time, its heat transfer rate is decreased due to increase the inlet temperature of the nanofluid where the temperature difference between the inlet and outlet of flowing fluids (deionized water and alumina nanofluid) is steadily increased from 8.00 am to 11.00 am, and then there is a fluctuation up to 4.00 pm. Both the inlet and an outlet temperature of nanofluid are varied depending upon solar radiation as shown in Fig. 7. Figure 8 shows the maximum temperature difference (23.3°C) which is reached at 11.00 am when the radiation is maximum.

Wind loss coefficient mainly depended on the wind speed and the thermal properties of air at ambient temperature. The variation of wind speed with respect to test time is shown in Fig. 9. The wind velocity is proportional to Reynolds number which has a direct effect on the Nu. Wind loss coefficient increased with increased wind speed. Up to 5.6 ms^{-1} speed, the wind power falls under the category of class 1 level and it is called poor wind. During the whole test period, the air velocity does not reach beyond this poor wind class. Radiation heat loss depends on the emissivity of the receiver material, ambient temperature, and receiver temperature which are the three parameters retaining the honest influence on radiation heat loss. The heat loss coefficient, radiation heat loss, and wind loss coefficient were fluctuating and reached the maximum values of 7.026, 8.134 and 51.32 $Wm^{-2}K^{-1}$ respectively as shown in Fig. 10. Heat loss from the collector system to the surrounding atmosphere by

all three modes of heat transfer are known as outside heat transfer coefficient, and it can be calculated by the product of heat loss coefficient and the temperature difference of surface-ambient.

The variation of inside heat transfer coefficient with bulk mean temperature for minimum and maximum fraction of nanofluid is shown in Fig. 11. The trend showed that the heat transfer coefficient is gradually increased and reached the maximum value of 634.5 $Wm^{-2}K^{-1}$ at 1.00 pm where the bulk mean temperature is 42.67°C. The optical efficiency also started from 31.57% minimum at 8.00 am and it is gradually increased to a maximum of 60.75% at 12.00 noon. It depends on the optical property of reflector and the intercept factor. For the maximum beam radiation of 821 Wm^{-2}, the total solar flux is 554.45 Wm^{-2}, but the highest value is 587.28 Wm^{-2} at 2.00 pm, where the receiver temperature is 130.20°C, as shown in Fig. 12. Solar flux is the quantity of solar radiation absorbed after overcoming the hurdles such as tilt factor, intercept factor, optical properties, receiver properties, and width of the aperture. The beam radiation, solar flux, and receiver temperature have increased positively up to noon time then gradually decreased in the opposite manner.

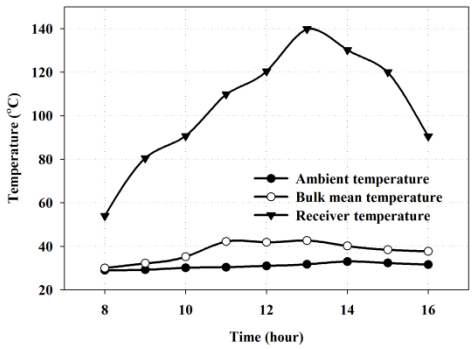

Figure 6. Temperatures with time

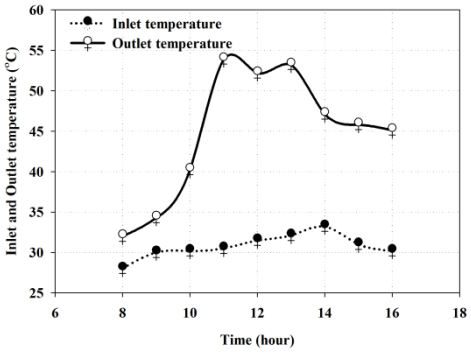

Figure 7. I/O temperature variations

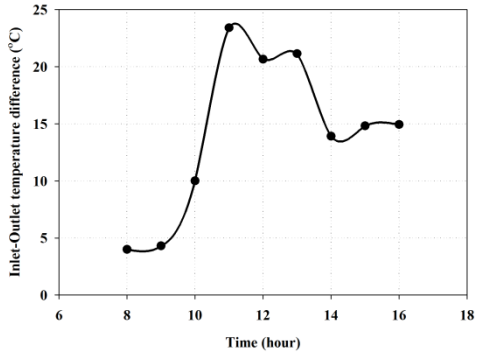

Figure 8. I/O temperature difference

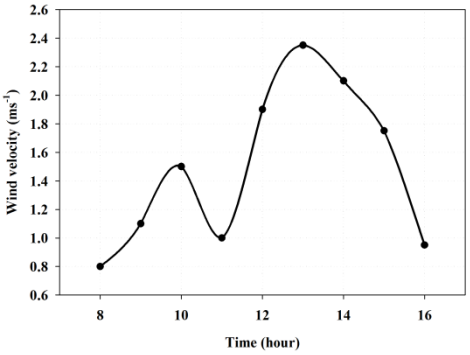

Figure 9. Variation of wind speed

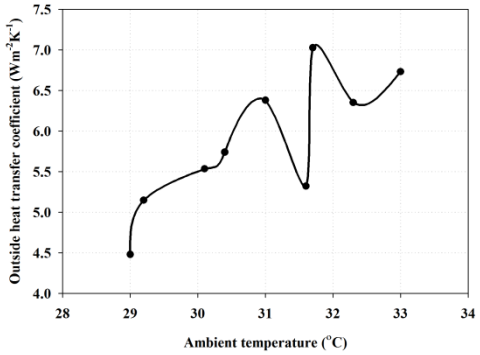

Figure 10. Outside heat transfer coefficient

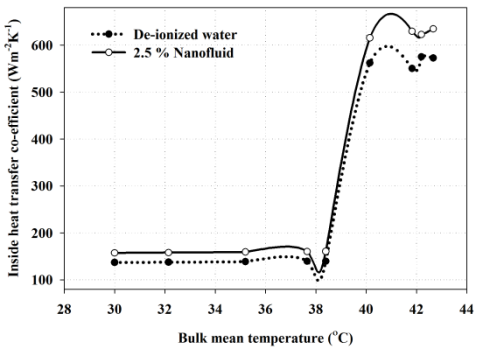

Figure 11. Inside heat transfer coefficient

The total loss coefficient range for the heat transfer fluid such as deionized water and alumina nanofluid uniformly increased from 30°C (4.342 $Wm^{-2}K^{-1}$) to 41.8°C (6.31 $Wm^{-2}K^{-1}$) as shown in Fig. 13. This loss coefficient between the two heat transfer fluids is in the range of negligible quantity. The flow slowly moved towards the turbulent type from the bulk mean temperature of 40°C (11.00 am). This rule is applicable for the given inner diameter (16.6 mm) of the receiver, mass flow rate (0.020 kgs^{-1}) of fluid and velocity of heat transfer fluid (0.09246 ms-1). The variation in temperature to the assumed turbulent flow depends on the internal diameter of the receiver, mass flow rate, and fluid velocity.

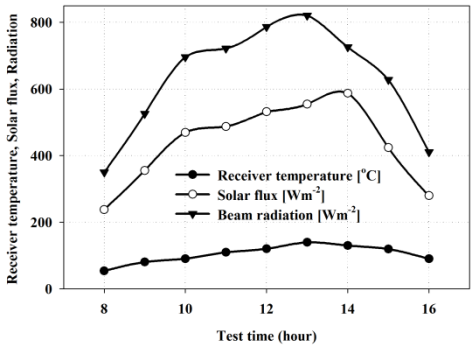

Figure 12. Parameters variation

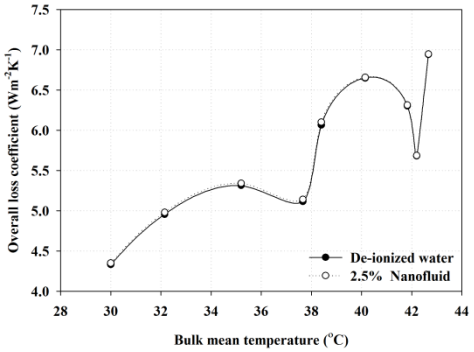

Figure 13. Overall loss coefficients

The useful heat gain increased with respect to the nanofluid concentration. The variation between the inlet temperature of heat transfer medium and ambient temperature had an influence on useful heat gain. The effect of volume fraction on useful heat gain is given in Fig. 14. The maximum possible useful heat gain can be obtained when the total collector system is maintained at the entry temperature of heat transfer fluid. As per the calculated data, the enhancement of collector efficiency is proportional to nanofluid volume fraction as shown in Fig. 15. The graph is plotted based on the average efficiency of the whole day for deionized water and 2.5% concentrations. This demonstrates a very good relation between nanofluid concentration and collector efficiency. The maximum instantaneous efficiency reached is 59.68% for 2.5% concentration. The collector efficiency increased parallel to the concentration of nanofluid. The thermal conductivity of nanofluid is higher than DI water. At the same time, the specific heat decreased with increased concentration.

The variation of instantaneous collector efficiency between the deionized water and nanofluid of 2.5% concentration is shown in Fig. 16. The heat transfer fluids are under turbulent region from 10.00 am to 3.00 pm and the rest of the test times are in the laminar flow region. The instantaneous collector efficiency slowly increased from 10.00 am to 3.00 pm due to its turbulent flow nature than other test times. The mass flow rates and concern velocities keep the fluid in the laminar region up to a certain temperature level. The calculated bulk mean temperature for the mass flow rate is 40°C. The bulk mean temperature of the heat transfer fluid is not allowed to increase beyond the given level to keep the flowing fluid in the laminar region. Due to the increase in the inside heat transfer coefficient at the turbulent region, the collector efficiency is enhanced. The variation in efficiency was observed for the defined heat transfer fluid from 12.00 noon to 1.00 pm. The instantaneous efficiency slowly decreased from 8.00 am to 10.00 am and then it reached to precise position due to its turbulent flow nature where

the inside heat transfer rate is high, 634.5 $Wm^{-2}K^{-1}$. By 11.00 am the PTC reached the high collector efficiency of 60.58%.

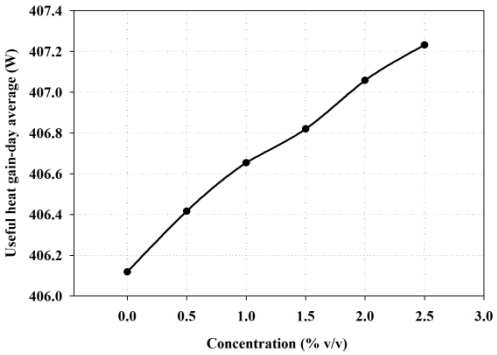

Figure 14. Useful heat gain

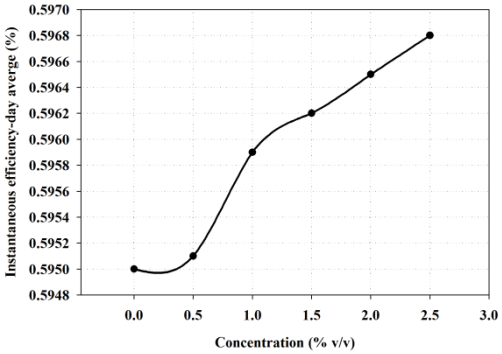

Figure 15. Efficiency on day average

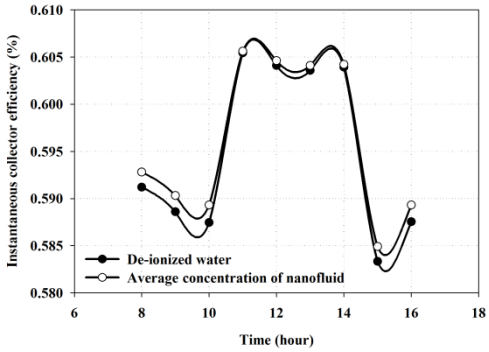

Figure 16. Efficiency of 0% and 2.5%

Conclusion

In the present work, the low-cost PTSC with hot water generation system for domestic purpose is designed and fabricated. The various volume fractions of aluminum oxide/deionized water such as from 0.5 to 2.5% are prepared by two-step method using magnetic stirrer and sonication. The experiments are carried out for nine hours from 8.00 am to 4.00 pm of test day. Al_2O_3 nanofluid is used as a heat transfer medium and it is allowed to flow through the copper receiver pipe. The maximum beam radiation is 821 Wm^{-2} and the average is 629.67 Wm^{-2}. The coefficient of wind loss, radiation loss, heat loss, overall loss, inside heat transfer, friction factor at the time of turbulent flow, collector efficiency factor, solar flux, useful heat gain, heat removal factor, collector capacitance factor and finally collector efficiency are also calculated based on day average as well as hourly basis. The instantaneous efficiency is increases parallel to useful heat gain. The efficiency of the collector and maximum heat gain is 59.68% and 467.231 W for 2.5% concentration on day average basis. On an hourly basis, it is observed that the peak value of efficiency and heat gain are 60.58% and 472.47 W. The efficiency enhancement was 3.90% than deionized water. The observation explained that the beam radiation had an influence on solar flux, heat removal factor, collector capacitance factor, and efficiency. On the other side, the overall heat loss is affected by heat loss coefficient and inside heat transfer coefficient for particular receiver material and size. The thermal properties of ambient air, wind velocity, receiver temperature and emissivity of receiver material had an effect on heat loss coefficient.

Nomenclature

A_a	- absorber area, [m^2]	np	- nanoparticle, [g]
CR	- concentration ratio (A_a/A_r), [-]	Nu	- Nusselt number, [-]
DI	- deionized, [-]	Pr	- Prandtl number, [-]
D_i	- inner diameter, [m^2]	Q_u	- useful heat gain, [W]
D_o	- outer diameter, [m^2]	R_b	- tilt factor, [-]
F_R	- heat removal factor, [-]	Re	- Reynolds number, [-]
h_{fi}	- heat transfer coefficient, [$Wm^{-2}K^{-1}$]	S	- solar flux, [Wm^{-2}]
h_r	- radiation loss coefficient, [$Wm^{-2}K^{-1}$]	T_a	- ambient temperature, (°C)
h_w	- wind loss coefficient, [$Wm^{-2}K^{-1}$]	T_{fi}	- fluid inlet temperature, (°C)
I_b	- solar radiation, [Wm^{-2}]	U_l	- heat loss coefficient, [$Wm^{-2}K^{-1}$]
K	- thermal conductivity, [$Wm^{-1}K^{-1}$]	U_o	- overall loss coefficient, [$Wm^{-2}K^{-1}$]
L	- aperture length, [mm]	W	- aperture width, [mm]

References

[1] Lippke, F., Direct Steam Generation in Parabolic Solar Power Plants: Numerical Investigation of the Transients and the Control of a Once-Through System, *J. Sol. Energy. Eng.*, *118* (1996), 2, pp. 9-14

[2] May, E.K., Murphy, L.M., Performance Benefits of the Direct Generation of Steam in Line-Focus Solar Collectors, *J. Sol. Energy. Eng.,105* (1983), 3, pp. 126-133

[3] Kalogirou, S., Lloyd, S., Use of Solar Parabolic Trough Collectors for Hot Water Production in Cyprus. A Feasibility Study, *Renewable Energy., 2* (1992), 2, pp. 117-124

[4] Kalogirou, S., Design and Performance Characteristics of a Parabolic-Trough Solar Collector System, *Appl. Energy., 47* (1994), pp. 341-354

[5] Vijayan, G., Karunakaran, R., Investigation of Heat Transfer Performance of Nanofluids on Conical Solar Collector under Dynamic Condition, *Adv. Mater. Res., 984-985* (2014), pp. 1125-1131

[6] Nour Chaabane., *et al*., Design and Performance of Trough Type Solar Collector for Domestic Use, *Proceedings,* Symposium on Stirling Cycle., Japan, 17 (2014), pp. 17-20

[7] Vijayan, G. and Karunakaran, R., Experimental Investigation on PTSC Hot Water Generation System**,** *J. Adv. Chem., 13* (2017), 3, pp. 1-16

[8] Markus, ECK., Heat Transfer Fluid for Future Parabolic Trough Solar Thermal Power Plants, *Proceedings***,** 4th ISES Solar World Congress on Solar Energy and Human Settlement., 2007, pp. 1806-1812

[9] Evangelos Bellos., *et al*., A Detailed Working Fluid Investigation for Solar Parabolic Trough Collector, *Appl. Therm. Eng., 11* (2016), pp. 1-27

[10] Vikrant Khullar., Himanshu Tyagi., Application of Nanofluid as the Working Fluid in Concentrating Parabolic Solar Collectors, *Proceedings,* 37th National & 4th International Conf. on Fluid Mechanics and Fluid Power., Chennai, India, 2010, vol. pp.

[11] Vikrant Khullar., *et al*., Solar Energy Harvesting Using Nanofluid Based Concentrating Solar Collector, *Proceedings, ASME*-3rd Micro/Nanoscale Heat & Mass Transfer International Conf., USA, 2012

[12] Alibakhsh Kasaeian., *et al*., Performance Evaluation and Nanofluid using Capability Study of a Solar Parabolic Trough Collector, *Energy Conservation and Management*., *89* (2015), pp. 368-375

[13] Qiyuan Li., *et al*., Experimental Investigation of a Nanofluid Absorber Employed in a Low Profile Concentrated Solar Thermal Collector, *Proceedings,* SPIE., *9668-9683* (2015), pp. 1-13

[14] Ghasemi, S.E., Ranjbar, A., Effect of Nanoparticles in Working Fluid on Thermal Performance of Solar Parabolic Trough Collector, *J. Mol. Liq.,* (2016), pp. 1-31

[15] Omid Karimi Sadaghiyani., *et al.,* The Effect and Combination of Wind Generated Rotation on Outlet Temperature and Heat Gain of LS-2 Parabolic Trough Solar Collector, *Thermal science., 17* (2013), 2, pp. 377-386

[16] Hachicha., *et al*., Heat Transfer Analysis and Numerical Simulation of a Parabolic Solar Collector, *Appl. Energy., 111* (2013), pp. 583-592

[17] Zhiyong Wu., *et al*., Three-Dimensional Numerical Study of Heat Transfer Characteristics of Parabolic Trough Receiver, *Appl. Energy., 113* (2014), pp. 902-911

[18] Gianluca Coccia., *et al*., Adoption of Nanofluids in Low Enthalpy Parabolic Trough Solar Collectors: Numerical Simulation of the Yearly Yield, *Energy Convers. Manage., 118* (2016), pp. 306-319

[19] Kaloudis, K., *et al*., Numerical Simulations of a Parabolic Trough Solar Collector with Nanofluid using Two Phase Model, *Renewable Energy., 97* (2016), pp. 218-229

[20] Natarajan., Srinivas, T., Experimental and Simulation Studies on a Novel Gravity based Passive Tracking System for a Linear Solar Concentrating Collector, *Renewable Energy., 105* (2017), pp. 312-323

[21] Syed Ameen Murtuza., *et al*., Experimental and Simulation Studies of Parabolic Trough Collector Design for obtaining Solar Energy, *Resour. Effic. Technol.,* (2017), pp. 1-8

[22] Weidong Huang., *et al*., Performance Simulation of a Parabolic Trough Solar Collector, *Sol. Energy., 86* (2012), pp. 746–755

[23] Men Wirz., Mathew Roesle., Three Dimensional, Optical and Thermal, Numerical Model of Solar Tubular Receiver in Parabolic Trough Concentrators, *J. Sol. Energy Eng., 134* (2012), pp. 1-9

[24] Ricardo Vasquag Padilla., *et al*., Heat Transfer Analysis of Parabolic Trough Solar Receiver, *Appl. Energy., 88* (2011), pp. 5097-5110

[25] De Risi, A., *et al*., Modeling and Optimization of Transparent Parabolic Trough Collector based on Gas-Phase Nanofluid, *Renewable Energy., 58* (2013), pp. 134-139

[26] Changfu you., *et al*., Modeling of Fluid Flow and Heat Transfer in Trough Solar Collector, *Appl. Therm. Eng., 54* (2013), pp. 247-254

[27] Valanarasu, A., Sornakumar, S., Theoretical Analysis and Experimental Verification of Parabolic Trough Solar Collector with Hot Water Generation System, *Therm. sci., 11* (2007), 1, pp. 119-126

[28] Sasa R. Pavlovic., *et al*., Design, Simulation and Optimization of Solar Dish Collector with Spiral Coil Thermal Absorber, *Therm. Sci., 20* (2016), 4, pp. 1387-1397

[29] Valanarasu, A., Sornakumar, S., Performance Characteristics of the Solar Parabolic Trough Collector with Hot Water Generation System, *Therm. Sci., 10* (2006), 2, pp. 167-174

[30] Velimir P. Stefanovic., *et al.*, Development and Investigation of Solar Collectors for Conversion of Solar Radiation into Heat and/or Electricity, *Therm. sci., 10* (2006), 4, pp.177-187

[31] Vijayan, G., Karunakaran, R., Characteristic Analysis of De-ionised Water and Ethylene Glycol based Aluminium Oxide Nanofluid, *J. Adv. Chem., 13* (2017), 5, pp. 6202-6207

[32] Rashmi, W., *et al.*, Preparation, Thermo-Physical Properties and Heat Transfer Enhancement of Nanofluids, *Mater. Res. Express., 1* (2014), 032001, pp. 2-48

[33] Suhaib Umer Ilyas., *et al.*, Preparation, Sedimentation and Agglomeration of Nanofluids, *Chem. Eng. & Technol., 37* (2014), 12, pp. 2011-2021

[34] Harwinder Singh., Pushpendra Singh., A Review Paper on Performance Improvement of Parabolic Trough Collector System, *J. Appl. Mech. Eng., 4* (2015), 2, pp. 1-10

[35] Kawira1, M., *et al.*, A Prototype Parabolic Trough Solar Concentrators for Steam Production, J. Agriculture, Sci. Technol., *14* (2012), 2, pp. 1-14

[36] Duffie, J.A., Beckman, W.A., *Solar Engineering of Thermal Processes,* John Wiley and Sons., New York, USA, (2006)

[37] Yogi Goswami, D., *Principles of Solar Engineering,* Taylor and Francis., USA, (2003)

[38] Sukhatme, S.P., *Solar Energy-Principles of Thermal Collection and Storage,* Tata McGraw-Hill Publishing Company Limited., New Delhi, (1994)